Single polarized Tm^{3+} laser in Zn-diffused $LiNbO_3$ channel waveguides

E. Cantelar,[a] J. A. Sanz-García, G. Lifante, and F. Cussó
Departamento de Física de Materiales, C-IV, Universidad Autónoma de Madrid, 28049 Madrid, Spain

P. L. Pernas
Departamento de Física Aplicada, C-XII, Universidad Autónoma de Madrid, 28049 Madrid, Spain

(Received 3 December 2004; accepted 16 February 2005; published online 15 April 2005)

In this work, laser operation at 1.76 μm in Tm^{3+}:$LiNbO_3$ Zn-diffused channel waveguides is reported. The laser emission is single polarized with the electric field parallel to the optic axis (π-polarization) and operates in continuous-wave regime, at room temperature. The threshold of laser oscillation is in the range of 40 mW, the slope efficiency is around 1%, and both magnitudes are dependent on the channel width, in accordance with the mode overlap between the pump and signal modes within the waveguides. © *2005 American Institute of Physics*.
[DOI: 10.1063/1.1887813]

Tm^{3+}-activated materials have been extensively investigated in the last years due to their broad infrared luminescence emissions, from 1400 nm up to 2100 nm (associated with $^3H_4 \rightarrow {}^3F_4$ and $^3F_4 \rightarrow {}^3H_6$ transitions), with potential interest in fields, such as *S*-band optical amplification, surgery, and remote sensing.[1–9] When rare-earth ions are incorporated into $LiNbO_3$, it is possible to combine the optical characteristics of the rare-earth ions with the electro-optic, acousto-optic, and nonlinear properties of $LiNbO_3$, together with the availability of well-developed techniques to fabricate low-loss channel waveguides.[10–14] Laser action of thulium-doped lithium niobate was first demonstrated in bulk material[1] and then in a guiding configuration using Ti-indiffused channel waveguides.[2] The observed stimulated emission was associated with the $^3F_4 \rightarrow {}^3H_6$ transition of Tm^{3+} ions, occurring at $\lambda_1 = 1.85$ μm in bulk, and simultaneously at $\lambda_1 = 1.85$ μm and $\lambda_2 = 1.81$ μm in the waveguide configuration. These two emissions correspond to Tm^{3+} transitions which are predominantly σ-polarized.[1,15]

In this work, we report π-polarized laser oscillation of Tm^{3+} ions, in Zn-diffused channel waveguides, operating in a slightly shorter-wavelength region, 1.76 μm, also corresponding to the $^3F_4 \rightarrow {}^3H_6$ Tm^{3+} transition. Laser oscillation is sustained in continuous-wave regime, at room temperature, without signs of photorefractive damage even in this π-polarized laser emission (electric field parallel to the optic axis), in accordance with previous reports of the high resistance to optical damage of Zn-diffused waveguides.[12,13]

Tm^{3+}-doped $LiNbO_3$ crystal has been grown by the Czochralski method. The content of Tm^{3+} in the initial melt was 2.0 mol %. The boule was oriented by Laue x-ray diffraction and then, slices perpendicularly to the *c* axis (z-cut samples) were cut and polished to optical quality. Zn diffusion has been used to fabricate the optical waveguides. Using this method, channel waveguides—having optical losses in the range of 0.3 dB/cm (at $\lambda = 1.55$ μm)—are fabricated.[16,17] In the present work, the ion exchange was carried out at 550 °C for 2 h, and then the sample was annealed at 850 °C for 4 h. During the ion exchange step, both sample surfaces are immersed in the Zn atmosphere and, therefore, a planar waveguide is simultaneously formed at the wafer surface opposite to the channel waveguides. M-line spectroscopic measurements performed in this planar waveguide, at 632.8 nm (He–Ne laser), showed that the waveguide supports three modes for transverse magnetic (TM) propagation (n_e—polarized modes) while only two modes, one of them close to cutoff, were found for transverse electric (TE) propagation (n_o—polarized modes). This situation is consistent with the existence of Gaussian index profiles for both refractive indices, with a depth of 6.5 μm, being the maximum index change of around 0.18% and 0.10%, for n_e and n_o polarization, respectively. According with these profiles, the waveguides are monomode both at the pump and laser wavelengths (795 nm, ordinary propagation, and 1.76 μm, extraordinary propagation, respectively).

A partial energy level diagram of Tm^{3+} ions in $LiNbO_3$ is sketched in Fig. 1. The excitation of Tm^{3+} ions can be efficiently performed by pumping in the dominant absorption band[15] ($^3H_6 \rightarrow {}^3H_4$ transition). From the $^3H_4$ manifold Tm^{3+} ions may relax by radiative transitions, giving fluorescence at around 0.8 μm and 1.45 μm ($^3H_4 \rightarrow {}^3H_6$ and $^3H_4 \rightarrow {}^3F_4$ transitions, respectively) or by nonradiative connection to the lower lying manifold ($^3H_5$) and then to the $^3F_4$ upper laser level.

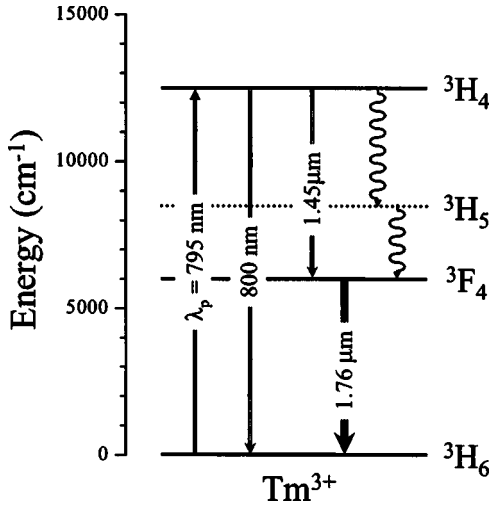

FIG. 1. Partial energy level diagram of Tm^{3+} ions indicating the main emissions observed after pumping at $\lambda_p = 795$ nm. Straight arrows indicate radiative transitions while wavy arrows represent nonradiative transitions.

[a]Electronic mail: eugenio.cantelar@uam.es

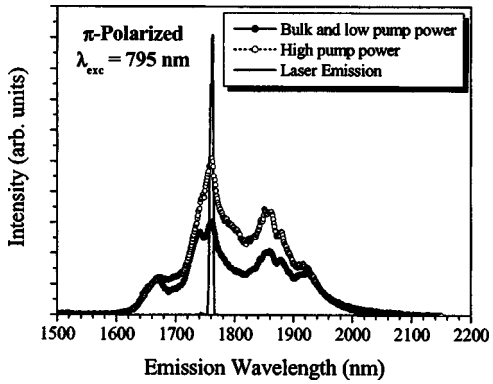

FIG. 2. Room-temperature π-polarized emission spectra associated to the $^3F_4 \rightarrow {}^3H_6$ Tm^{3+} transition measured in different experimental conditions: Bulk or low pump power waveguide emission (full circles), waveguide emission at high pumping levels (open circles), and waveguide laser emission (continuous line).

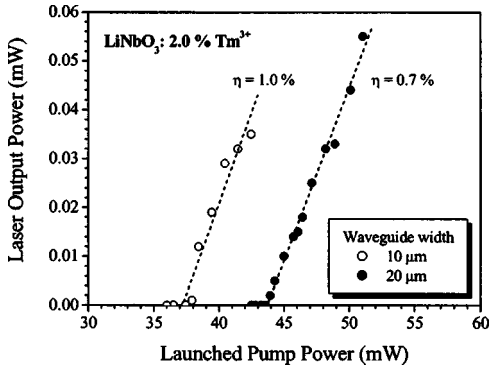

FIG. 3. Output efficiency curves measured in 10 μm and 20 μm width channel waveguides (open and full circles, respectively).

Optical excitation of the channel waveguides (8.5 mm length) was performed by end-fired coupling a Ti:Sapphire laser, operating at 795 nm, by using a microscope objective. The geometry of the experiment was adopted to launch TE propagating modes into the channel waveguides, in order to match the electric-field orientation suitable for Tm^{3+} excitation, according to the dominant polarization character of the $^3H_6 \rightarrow {}^3H_4$ transition. The luminescence from the waveguide was collected at the opposite end with a second microscope objective and then dispersed by using an ARC monochromator (SpectraPro-500i). The luminescence was detected with a cooled InAs detector.

The π-polarized emission spectrum associated with the $^3F_4 \rightarrow {}^3H_6$ Tm^{3+} transition, recorded under different experimental conditions, is presented in Fig. 2. Full circles represent the emission from the waveguide at low pump power, which is coincident with that observed for bulk $LiNbO_3$:Tm^{3+}. Open circles correspond to the waveguide emission at higher pumping levels. As it can be seen, the feedback provided by Fresnel reflections at the endfaces is high enough to produce detectable amplified spontaneous emission, giving rise to distortions in the luminescence spectrum. Nevertheless, it was impossible to attain laser oscillation with the feedback provided only by Fresnel reflections ($R \approx 14\%$). Lasing was achieved by forming a laser cavity: A high reflector ($T=92\%$ @ 795 nm, $R \geqslant 99\%$ @ 1.6 μm $< \lambda < 2.0$ μm) was attached to the entrance endface, while a partially reflective output coupler ($R \geqslant 99.8\%$ @ 795 nm, $R \approx 95\%$ @ 1.6 μm $< \lambda < 2.0$ μm) was used at the other end. Under these experimental conditions, laser emission centered at 1762.6 nm with a full width at half maximum around 8.0 nm is detected (continuous line in Fig. 2). This lasing wavelength is slightly shorter than that reported in previous $LiNbO_3$:Tm^{3+} lasers ($\lambda = 1.81$ μm and 1.85 μm).[1,2]

Figure 3 shows the output efficiency curves measured in 10 μm and 20 μm width channel waveguides. The power of the pump and signal beams were measured by using a Thorlabs power meter. As it can be observed, the launched pump power required for reaching threshold was 37 mW and 43 mW for the 10 μm and 20 μm width channel waveguides, respectively, while the slope efficiency was estimated to be between 0.7% and 1.0%, similar to those values reported for Ti-indiffused Tm^{3+} waveguide lasers.[2] The increase observed in the threshold of laser operation with the channel width can be related with differences in the mode overlap between pump and signal modes in the waveguides. The threshold power (P_{th}) for a quasi-three-level laser can be expressed as:[18]

$$P_{th} = \frac{h\nu_p(L_i + T + 2N_1^0\sigma\ell)}{2\eta_p\eta_a(f_1 + f_2)\sigma\tau_f}\left[\frac{V_{eff}}{nl}\right], \quad (1)$$

where $h\nu_p$ represents the pump photon energy, η_p is the pump quantum efficiency, η_a is the absorption efficiency for

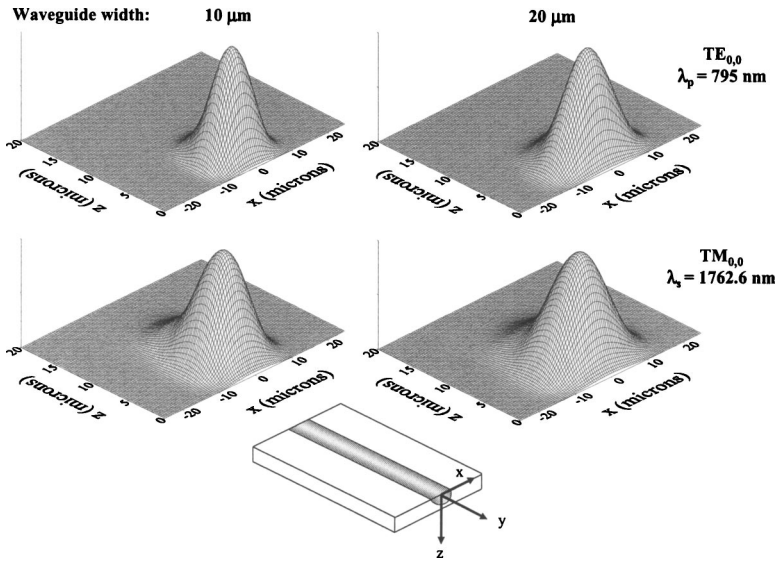

FIG. 4. Calculated modal intensity distributions at pump ($TE_{0,0}$) and signal wavelengths ($TM_{0,0}$) in the 10 μm and 20 μm width channel waveguides. The diagram in the lower part of the figure indicates the coordinate reference system.

pump power, f_1 and f_2 are the fractional population in the lower and upper laser Stark components, respectively, σ is the gain cross section, τ_f is the lifetime of the upper manifold, L_i are the intrinsic cavity losses, T is the transmission of the output coupler, N_1^0 the unpumped population inversion density, l is the length of the waveguide, n is the effective refractive index, and V_{eff} symbolizes the effective mode volume.[18]

The different spectroscopic parameters involved in Eq. (1) are independent of the waveguide channel width and, assuming that the intrinsic losses are also similar, the ratio between threshold values for both waveguides depends exclusively on the relation between the corresponding effective mode volumes:

$$\frac{P_{\text{th}}(10\ \mu\text{m})}{P_{\text{th}}(20\ \mu\text{m})} = \frac{V_{\text{eff}}(10\ \mu\text{m})}{V_{\text{eff}}(20\ \mu\text{m})}. \tag{2}$$

The effective mode volumes can be evaluated from the modal intensity distribution by integration over the cross section area, A, of the active region:

$$\frac{V_{\text{eff}}}{nl} = \frac{\int\int_A r_p(x,z)dxdz \int\int_A \Phi_0(x,z)dxdz}{n\int\int_A r_p(x,z)\Phi_0(x,z)dxdz}. \tag{3}$$

The corresponding pump and signal modes, $TE_{0,0}$ and $TM_{0,0}$, in the 10 μm and 20 μm width channel waveguides have been calculated either by the effective index method[19] or by the imaginary propagation method,[20] with identical results. From these modal distributions (Fig. 4), the calculated ratio between the effective volumes was found to be $V_{\text{eff}}(10\ \mu\text{m})/V_{\text{eff}}(20\ \mu\text{m}) = 0.76$, which is in good agreement with the experimental value $P_{\text{th}}(10\ \mu\text{m})/P_{\text{th}}(20\ \mu\text{m}) = 0.84$.

As it has been indicated above, the laser emission is fully π-polarized, which is in contrast with the σ-polarization character previously reported for laser emission in $Tm^{3+}:LiNbO_3$ lasers.[1,2] This fact, together with the slightly different lasing wavelength, clearly indicates that, in this case, the laser transition involves different Stark components of the $^3F_4$ and $^3H_6$ Tm^{3+} manifolds.[1,15] The selection of a π-polarized laser emission may become advantageous for nonlinear applications via quasi-phase matching in periodically poled $LiNbO_3$, making possible then to take advantage of the highest nonlinear coefficient (d_{33}) of the crystal.[21,22] Let us finally indicate that the temperatures needed to carry out Zn diffusion are sufficiently low to preserve domain structures already present in the wafers[23] which can then be previously defined, by a variety of different techniques, increasing the versatility of the fabrication procedure.

Work partially supported by Ministerio de Ciencia y Tecnología and Comunidad de Madrid (Spain) under Project Nos. TIC2002-0147 and GR-MAT-0108-2004.

[1] L. F. Johnson and A. A. Ballman, J. Appl. Phys. **40**, 297 (1969).
[2] J. P. de Sandro, J. K. Jones, D. P. Shepherd, M. Hempstead, J. Wang, and A. C. Tropper, IEEE Photonics Technol. Lett. **8**, 209 (1996).
[3] R. C. Stoneman and L. Esterowitz, IEEE J. Sel. Top. Quantum Electron. **1**, 78 (1995).
[4] V. Sudesh and J. A. Piper, IEEE J. Quantum Electron. **36**, 879 (2000).
[5] T. Kamatsu, Y. Yano, and T. Ono, IEEE Photonics Technol. Lett. **13**, 31 (2001).
[6] L. N. Ng, E. R. Taylor, and J. Nilsson, Electron. Lett. **38**, 1246 (2002).
[7] J. I. Mackenzie, C. Li, D. P. Shepherd, R. J. Beach, and S. C. Mitchell, IEEE J. Quantum Electron. **38**, 222 (2002).
[8] K. Sasagawa, Z. Yonezawa, R. Iwai, J. Ohta, and M. Nunoshita, Appl. Phys. Lett. **85**, 4325 (2004).
[9] S. Agger, J. H. Povlsen, and P. Varming, Opt. Lett. **29**, 1503 (2004).
[10] L. Chanvillard, P. Aschieri, P. Balde, D. B. Ostrowsky, M. de Micheli, L. Huang, and D. J. Bamford, Appl. Phys. Lett. **76**, 1089 (2000).
[11] B. K. Das, H. Suche, and W. Sohler, Appl. Phys. B: Lasers Opt. **73**, 439 (2001).
[12] W. M. Young, R. S. Feigelson, M. M. Fejer, M. J. F. Digonnet, and H. J. Shaw, Opt. Lett. **16**, 995 (1991).
[13] W. M. Young, M. M. Fejer, M. J. F. Digonnet, A. F. Marshall, and R. S. Feigelson, J. Lightwave Technol. **10**, 1238 (1992).
[14] M. Fujimura, A. Shiratsuki, T. Suhara, and H. Nishihara, Jpn. J. Appl. Phys., Part 2 **37**, L659 (1998).
[15] L. Núñez, J. O. Tocho, J. A. Sanz-García, E. Rodríguez, F. Cussó, D. C. Hanna, A. C. Tropper, and A. C. Large, J. Lumin. **55**, 253 (1993).
[16] R. Nevado and G. Lifante, Appl. Phys. A: Mater. Sci. Process. **72**, 725 (2001).
[17] P. L. Pernas, M. J. Hernández, E. Ruíz, E. Cantelar, R. Nevado, C. Morán, G. Lifante, and F. Cussó, Appl. Surf. Sci. **161**, 123 (2000).
[18] T. Taira, W. M. Tulloch, and R. L. Byer, Appl. Opt. **36**, 1867 (1997).
[19] G. Lifante, *Integrated Photonics* (Wiley, Chichester, England, 2003).
[20] S. Jungling and J. C. Chen, IEEE J. Quantum Electron. **30**, 2098 (1994).
[21] M. M. Fejer, G. A. Magel, D. H. Jundt, and R. L. Byer, IEEE J. Quantum Electron. **28**, 2631 (1992).
[22] V. Pruneri, S. Butterworth, and D. C. Hanna, Appl. Phys. Lett. **69**, 1029 (1996).
[23] E. Cantelar, G. A. Torchia, J. A. Sanz-García, P. L. Pernas, G. Lifante, and F. Cussó, Appl. Phys. Lett. **83**, 2991 (2003).